GeoScienceWorld
Lithosphere
Volume 2024, Article ID lithosphere_2023_320, 17 pages
https://doi.org/10.2113/2024/lithosphere_2023_320

Lithosphere

Research Article

Study of the Effect of Drying and Wetting Cycles and Water Content on the Shear Characteristics of Tailing Sands

Yakun Tian,[1,2] **Zhijun Zhang**,[1,2] **Min Wang**,[1] **Lingling Wu**,[1,2] **Lin Hu**,[1,2] **and Rong Gui**[1,2]

[1]*School of Resource & Environment and Safety Engineering, University of South China, Hengyang, 421001, China*
[2]*Hunan Province Engineering Technology Research Center for Disaster Prediction and Control on Mining Geotechnical Engineering, Hengyang , 421001, China*

Correspondence should be addressed to Min Wang; wangmin@usc.edu.cn

Received 26 October 2023; Accepted 21 February 2024; Published 8 March 2024

Academic Editor: Yuqi Wu

The mechanical characteristics of tailing sands have an important impact on the safety and stability of the tailing dams. Fully understanding the effect of drying and wetting cycles (DWC) and water content on the characteristics of tailing sands is urgently needed. In this study, direct shear tests were first carried out to analyze the effect of DWC and water content on the macroscopic mechanical characteristics of tailing sands. Then, the mesoscopic mechanical behavior of tailing sands with different water contents under the action of DWC was studied by using PFC^{2D} particle flow software. The results showed that the effect of DWC on the shear properties of tailing sands is more pronounced than water content. The cohesive force and the internal friction angle increase first and then decrease with the increasing water content. With the increasing number of DWC, the cohesive force and the internal friction angle all decreased to varying degrees. The results of the mesoscopic mechanical analysis indicated that after experiencing the DWC, the force chain of the sample gradually thickens to form a coarse force chain network area, and the number of cracks inside the sample is significantly larger than that of the sample that has not experienced the DWC. The results of this study are of great significance for understanding the macroscopic and mesoscopic shear failure mechanism of tailing sands under the effects of DWCs and water content.

1. Introduction

The tailing dam is a man-made debris flow hazard with high potential energy, and there are many unstable factors in its operation process. The collapse of the tailing dam not only affects the production of mining enterprises but also brings huge disasters to the inhabitants. Due to periodic changes in water conditions (i.e., rainfall infiltration, water evaporation, and repeated elevation and decline of the infiltration line), the tailing dam is subjected to long-term drying and wetting cycles (DWCs) during operation. It was found that the DWCs will lead to a decrease in the mechanical properties of the soil, and the changes in water content also affect the microstructure and mechanical properties of the soil. Under the action of DWC and water content, the matric suction and shear strength of the soil will change, thus affecting the stability of the soil structure. Therefore, a comprehensive understanding of the influence of the DWC and water content on the characteristics of tailing sands is of great significance for the long-term safety and stability of the tailing dam.

A substantial effort has been made on the changes in the physical properties and mechanical behavior of rock materials under the action of cyclic wetting and drying [1–21]. The properties of rock materials (i.e., porosity, longitudinal wave velocity, compressive strength, shear strength, etc.) are significantly influenced by DWCs. Zhou et al. [7] studied the dynamic tensile strength characteristics of rocks after cyclic drying and wetting. They inferred that the cumulative crack damage caused by cyclic drying and wetting was the main reason for the reduction of strength. Zhao et al. [8] carried out nuclear magnetic resonance (NMR) tests and mechanical tests of mudstone under the action of cyclic drying and wetting. It indicated that

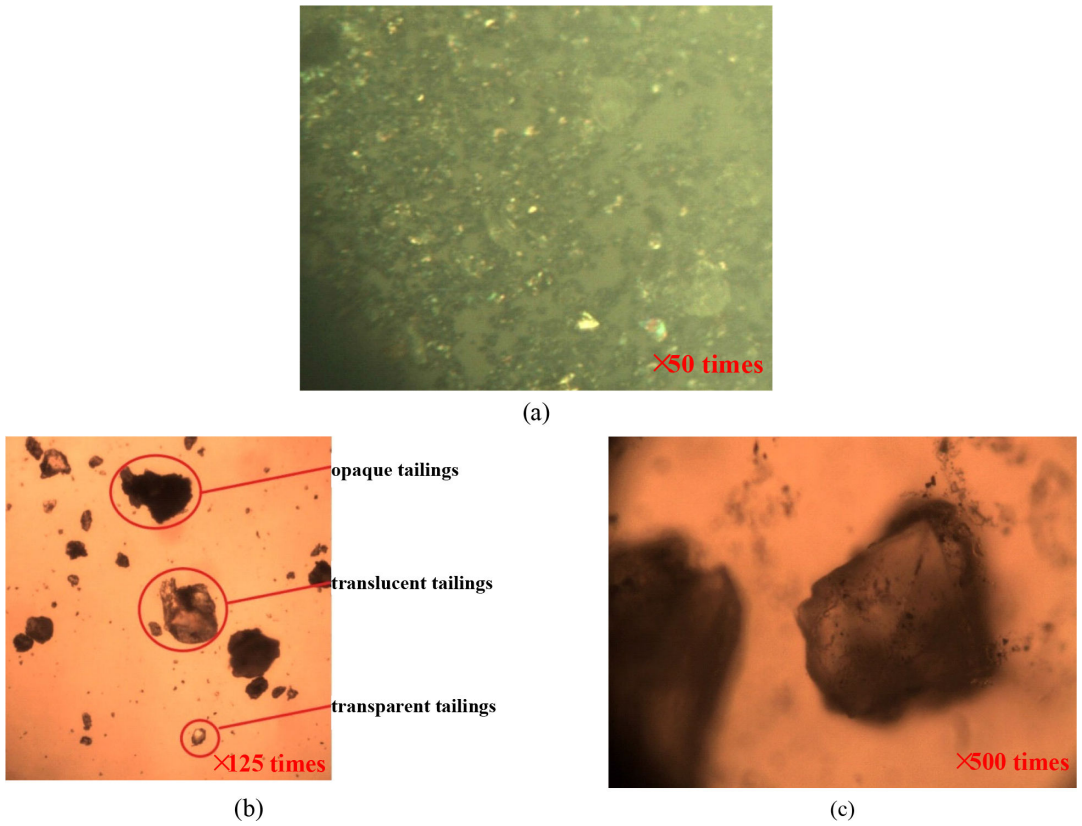

Figure 1: The polarizing microscope image of tailing sands. (a) 50 times transmitted light image of tailing sands; (b) 125 times transmitted light image of tailing sands; and (c) 500 times transmitted light image of tailing sands.

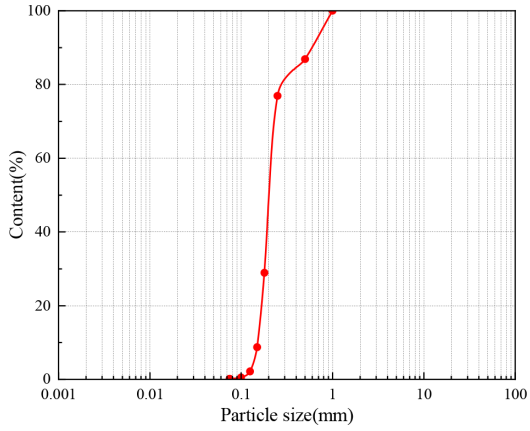

Figure 2: The cumulative curve of particle size distribution of tailing sands.

the increase in porosity was responsible for the deterioration of the mechanical properties of mudstone. Huang et al. [9] reported that the damage of uniaxial compressive strength and elastic modulus of sandstone has a logarithmic relationship with the number of DWCs. Li et al. [13] found that the strength and deformation characteristics of the medium-grained sandstone samples decreased with the increase in the DWCs. Wu et al. [16] investigated the effect of DWC on the physical characteristics and strength parameters of silty mudstone and silty sandstone. They suggested that the mechanism of cyclic drying and wetting-induced rock weakening is mainly microcrack expansion caused by contraction and expansion of the mineral structure. Yao et al. [17] found that the uniaxial compressive strength and tensile strength of argillaceous siltstone in the Yangtze River Basin decreased exponentially with the number of DWC. The composition and microstructure of minerals showed gradual changes under the action of DWCs. Li et al. [18] explored the effect of DWCs on sandstone properties (i.e., porosity, dynamic strength, and energy dissipation). It was found that the effect of water saturation on dynamic strength changed from enhanced to weakened with the increase in porosity. Except for physical properties and strength characteristics, the fracture toughness has also been investigated. For example, Hua et al. [19] and Ying et al. [20] found that the fracture toughness decreased with increasing number of DWCs. Cai et al. [21] explored the fracture behavior of sandstone subjected to DWCs. It indicated that the fracture toughness and energy dissipation of sandstone decreased significantly with the increasing number of drying and wetting cycles.

The DWCs play an important role in soil physical and mechanical properties. A number of scholars have carried out studies on the physical and mechanical properties of soils under the action of wet and dry cycles [22–28]. It was found that the DWCs can cause the changes in particle position and pore structure of soil, which ultimately causes changes in shear strength. As the number of drying

Figure 3: Tailing sands samples with different water contents.

of tailing sands is an important mechanical parameter to evaluate the stability of tailing dam. The investigations about the effect of DWCs on shear properties of tailing sands are still insufficient. To comprehensively evaluate the safety and stability of tailings dams and effectively control the hazard of tailings dam failure, it is necessary to investigate the effects of DWCs on the shear mechanical properties of tailing sands.

During the accumulation and destruction of tailing dam, the formation mechanism of local or overall shear zones depends on the mesoscopic mechanical characteristics of tailings. Simulation of geotechnical materials under various stress states in nature with discrete element particle flow models is an important method to obtain mesoscopic mechanical parameters. In this study, a lead-zinc tailing in Hunan Province, China was taken as the research object. First, tailing sands samples with different water content

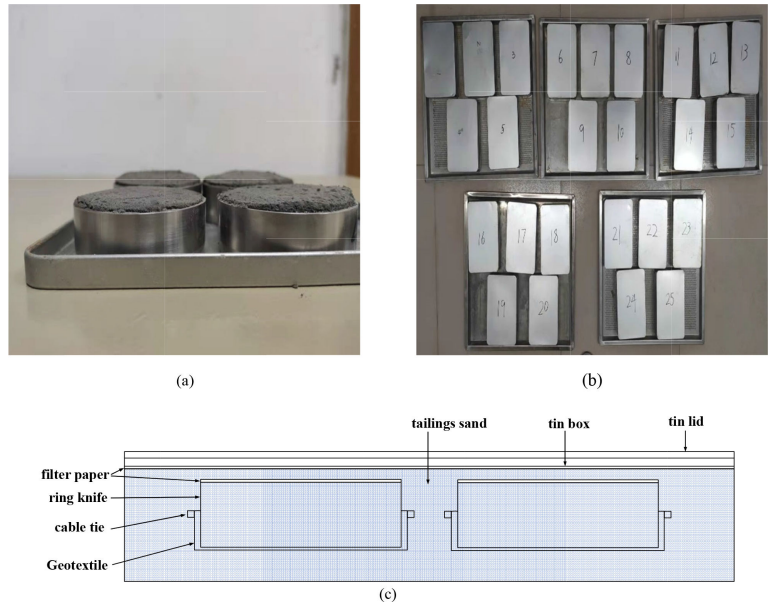

Figure 4: The cyclic drying and wetting test device.

and wetting cycles increases, the water stability of soil aggregates decreases [25]. The soil microstructure, such as particle shape, size, arrangement and distribution, and pore connectivity, closely affect the macroscopic characteristics [28, 29]. Hafhouf et al. [24] studied the effects of DWCs on the unconfined compressive strength of Algerian soil. Tang et al. [25, 27] carried out a study on the mechanical properties of unsaturated soil under the action of DWCs. It was found that the cyclic drying and wetting increased the number of cracks and reduced the brittleness of the soil, which eventually led to the decrease in soil strength. The tailing sands is a kind of unsaturated soil. Research shows that the drying and wetting cycles increase cracks in unsaturated soils, and significantly change the hydraulic behavior of the soil [26]. The cracks promote the formation of damage zones in the soil which leads to the reduction of the shear strength [30, 31]. Wang et al. [32] revealed that the microstructure deformation of tailing sands is the main factor contributing to tailings leakage. The shear strength under the action of DWCs were prepared and the influence of water content and cyclic drying and wetting on the macroscopic shear mechanical parameters of the tailing sands was explored. Then, the PFC^{2D} particle flow simulation method was used to further analyze the evolutionary law of mesoscopic properties, such as the contact network between particles, the number of cracks, and the failure mode, under the action of water content and DWCs. It has certain theoretical significance and engineering value for the innovation and development of stability analysis methods for tailing dam.

2. Materials and Methods

2.1. The Physical Properties of Tailing Sands. In this study, the lead-zinc tailing sands from a tailing dam in Hunan Province, China were selected, and the obtained samples were brought back to the laboratory after being sealed and

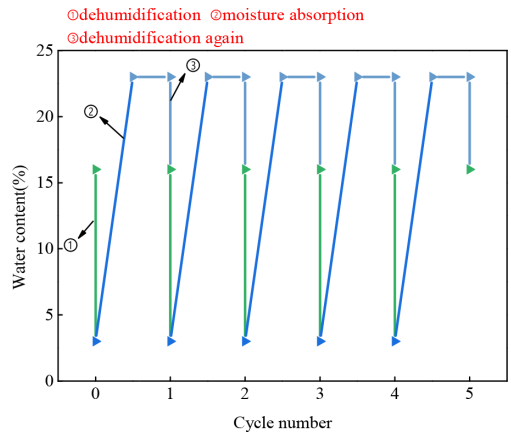

Figure 5: The process of drying and wetting cycles.

Figure 6: The direct shear experiment of tailing sands sample.

are distributed in blocks and have obvious powdery debris on the surface.

The natural density of the tailing sands is 1.734 g/cm^3 measured by the ring knife method, and the natural water content is determined to be 10% by the drying test. In addition, the optimal water content test and the specific gravity test were carried out in sequence according to relevant standards. The physical parameters such as density, optimal water content, specific gravity, and porosity obtained from the test are shown in Table 1. The particle size of soil and its composition play a decisive role in the mechanical properties. The particle size is generally characterized by gradation. In the tailing sands samples taken for this test, more than 90% of the particles have a particle size greater than 0.075 mm, so the sieving method was selected to carry out the particle analysis test.

Eight samples of 400 g tailing sands were taken for parallel sieving tests, and the cumulative curve of particle size distribution was obtained as shown in Figure 2. The particle gradation parameters of the sample are shown in Table 2. It can be seen that the unevenness coefficient (Cu) is 1.37 and the curvature coefficient (Cc) is 1.04 which do not meet the requirements of Cu ≥ 5 and Cc = 1–3. Therefore, the tailing sands sample is poor gradation.

2.2 Sample Preparation. To completely remove the water from the tailing sands, the collected tailing sands were dried in a drying oven at a temperature of 120°C until no further change in mass occurred. According to the natural and optimal water content of the tailing sands, the dried tailing sands were added with water to prepare samples with different water contents (10%, 12%, 14%, 16%, and 18%). The prepared tailing sands were then placed in a sealed bag

Table 1: Basic physical parameters of tailing sands.

Natural dry density, ρ_d (g cm^{-3})	Natural water content, ω_{op} (%)	Optimal water content, ω (%)	Proportion, G_s	Porosity
1.734	10%	16%	2.66	0.517

numbered. The tailing sands has the characteristics of fine particles and low viscosity. It does not agglomerate when soaked in water, and has a frosty and grainy feeling when touched by hand. The XPL-2 transflective polarizing microscope was used to observe the apparent structure of the samples. From the reflected light image of the lead-zinc tailing sands (Figure 1(a)), it can be seen that the particles have obvious metallic luster. Under 125 times transmitted light (Figure 1(b)), the tailings can be divided into opaque tailings, translucent tailings, and transparent tailings according to the light transmittance. The lead-zinc tailings are predominantly opaque tailings with many powdery debris. Studies have shown that particles with powdery debris will increase the cohesion and internal friction angle of tailings under the action of water [33].

From the 500 times transmitted light image (Figure 1(c)), it can be observed that the lead-zinc tailing sands are mostly mixed mineral particles and metal mineral particles, which

and kept for 24 hours to fully integrate with water. The prepared samples with different water contents are shown in Figure 3.

2.3. Experimental Strategy. To fully simulate the DWCs on site, the tailing sands samples were compacted in three layers into a ring knife with a size of Φ61.8 mm × 20 mm before the DWCs. The bottom of the ring knife was wrapped with a sand-stopping and water-permeable geotextile and fixed with a cable tie, while the upper part of the ring knife was covered with filter paper and plastic wrap to prevent water loss. First, spread a layer of prepared tailing sands on the bottom of the iron box with a size of 188 mm × 138 mm × 38 mm and compact it. Then, put the ring knife sample on the second layer and fill the gap with tailing sands at the same time. Finally, fill the tailing sands above the ring knife sample and compact it again. Seal the iron box and let it stand for

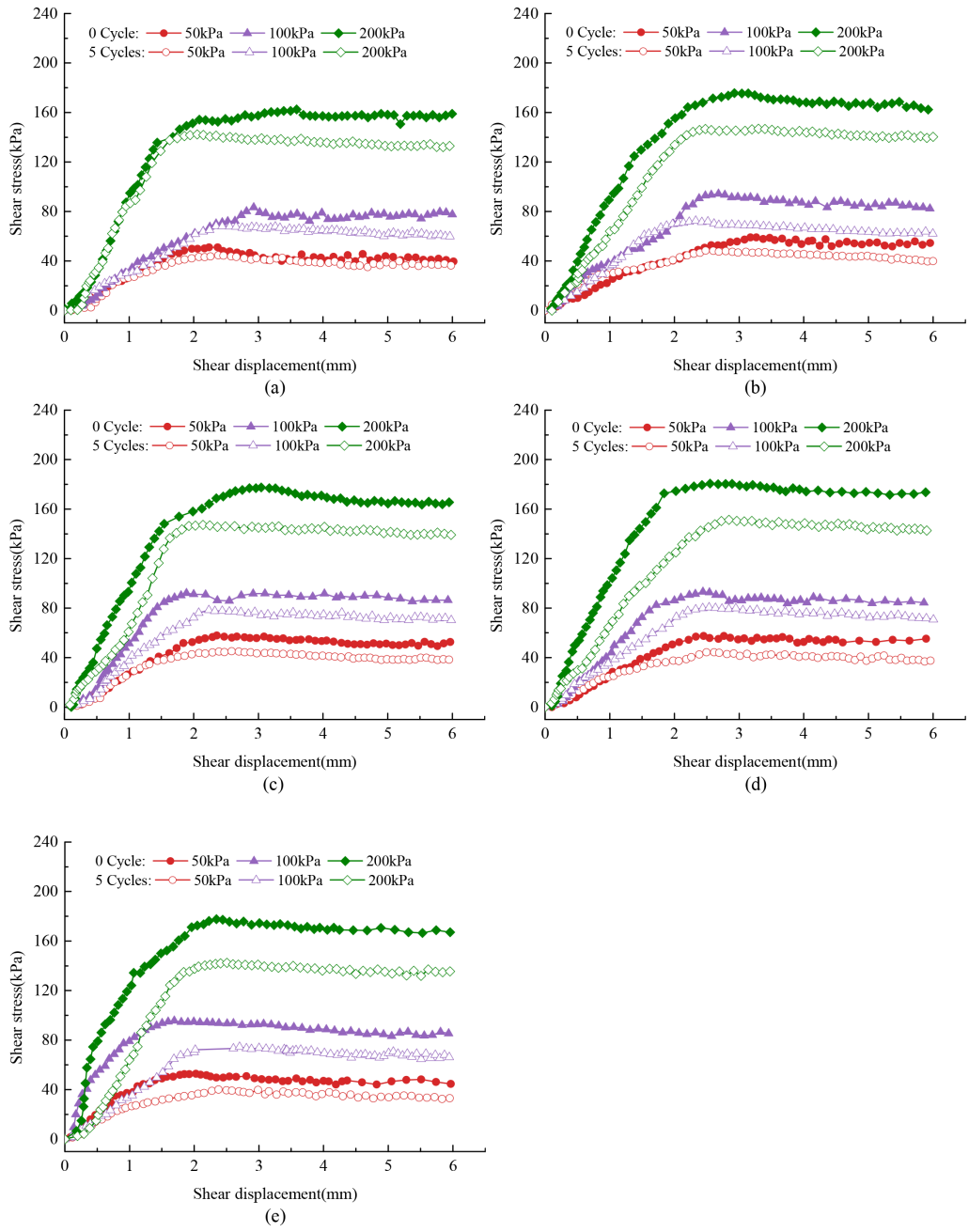

Figure 7: The shear stress and displacement curves of tailing sands samples that experienced 0 drying and wetting cycle and 5 drying and wetting cycles. (a) 10% water content; (b) 12% water content; (c) 14% water content; (d) 16% water content; and (e) 18% water content.

Table 2: Grading parameters of tailing sands.

Effective particle size d_{10} (mm)	Median particle size d_{30} (mm)	Restricted particle size d_{60} (mm)	Inhomogeneity coefficient (C_u)	Curvature coefficient (C_c)
0.152	0.181	0.208	1.37	1.04

72 hours. This method can not only effectively avoid the disturbance of adding water on the surface of the sample in the process of DWCs but also eliminate the interference of human factors in the sampling process. Figure 4 shows the cyclic drying and wetting device.

In the pre-experiment, it was found that after 5 DWCs, the mechanical properties of tailing sands tended to be stable and showed a certain regularity. In this study, the samples with different water content were set up to experience 1, 2, 3, 4, and 5 times of DWCs. A group of control tests that did not experience the DWCs was set up at the same time. There are 3 parallel tests in each group, and the result is the average value of the three tests. The

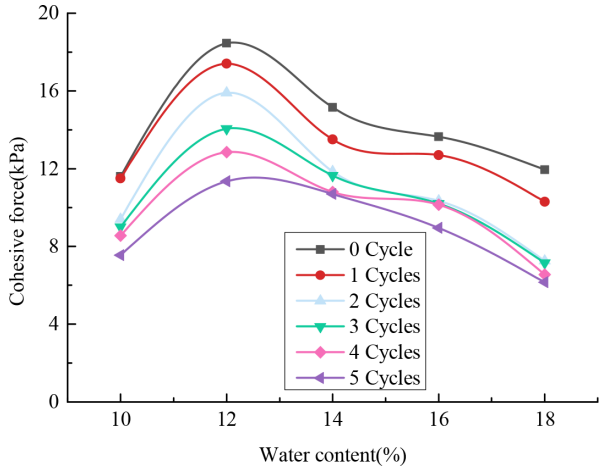

Figure 8: The cohesion force of tailing sands samples with different water content subjected to drying and wetting cycles.

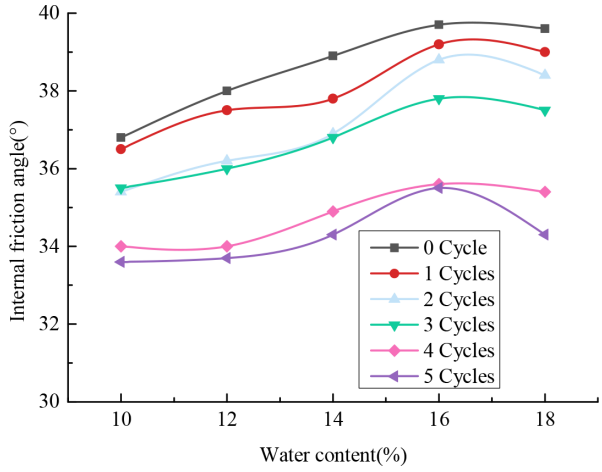

Figure 9: The internal friction angle of tailing sands samples with different water content subjected to drying and wetting cycles.

process of DWC in natural environment was simulated by low-temperature drying and artificial watering. According to the natural environment of the site, it is determined that the variation range of the water content during the DWCs is controlled between 3% and 23%. The DWCs process is shown in Figure 5 (take the water content of 16% as an example).

After each DWC, the prepared sample was installed on the test apparatus according to the shear test procedure. Note that after the sample installation, a wet cotton with same water content was used to surround the container. The load sequence was set to 50, 100, and 200 kPa. To avoid the change in water content during the test, the shear rate was selected as 0.8 mm/min, and the method of consolidation fast shear was used. The direct shear test process is shown in Figure 6.

3. Results and Analysis

3.1. Relationship between Shear Stress and Displacement. With vertical loads of 50, 100, and 200 kPa, the shear stress and displacement relationship curves of tailing sands with different water contents under DWCs were obtained. Due to space limitations, only the shear stress and displacement relationship curves of tailing sands that experienced 0 DWCs and 5 DWCs (Figure 7) are listed. It is observed that the shear stress and displacement relationship curve of tailing sands can be divided into 3 stages: elastic stage, peak stage, and stable stage. In the elastic stage, as the vertical load increases, the relationship curve between shear stress and displacement becomes steeper, indicating that the initial shear modulus of the tailing sands is positively correlated with the applied vertical load. At the peak stage, the maximum value of the shear stress occurs, and the bonding between the particles reaches the maximum at this time. In the stable stage, as the displacement increases, the shear stress no longer changes greatly or even shows a downward trend, indicating that the sample has reached the shear strength. At this time, the sample has been destroyed, which can also be called the failure stage.

Under the condition of the same water content and the same vertical load, the shear strength of the tailing sands decreased and the shear displacement corresponding to the shear strength became smaller after 5 cyclic drying and wetting. It indicated that cyclic drying and wetting changes the mechanical properties of the tailing sands and shortens the elastic deformation stage. It makes the sample reach the shear strength faster and then enter the stable stage.

The above phenomenon is attributed to the fact that the evaporation and accumulation of water change the original pore structure of the sample during the DWC process. A slight expansion of the sample volume after cyclic drying and wetting was also found in the experiment. Under the action of DWCs, the pores within the sample increase, and the original particle cements are separated into dispersed particles. The strength of the sample is maintained by the bound water and particles between pores. In the direct shear test, the strength of the brittle particles is low, so that the sample becomes more easily to be destroyed under the same vertical load.

Under the condition of the same number of cycles, the effect of water content on the shear strength is not obvious, especially when the vertical load is 50 kPa. In most cases, the shear strength of sample with 16% water content is higher than that with other water content. The shear strength does not increase by the same multiple as the vertical load increase.

3.2. Cohesion Force and Internal Friction Angle. It can be seen from the shear stress and displacement relationship curves that both cyclic drying and wetting and water content have an effect on the shear strength of tailing sands. To further analyze the effects of the DWCs and water content on the shear characteristics of tailing sands, it is necessary to investigate the variation laws of the cohesion force and internal friction angle of tailing sands. Taking the normal stress δ as the horizontal axis and the shear stress τ as the vertical axis, the cohesion force and internal friction angle were obtained by fitting the data of the shear strength curve through Coulomb's law.

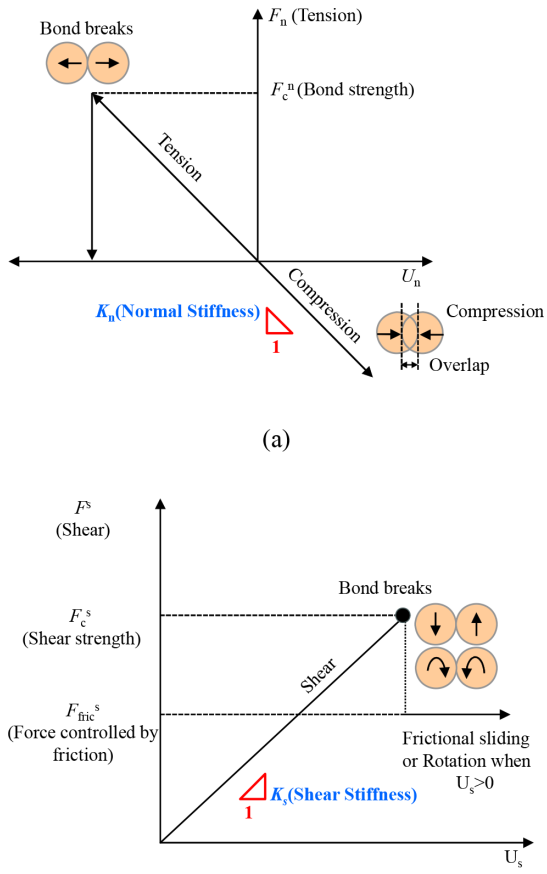

FIGURE 10: Constitutive behavior for parallel bonded particle model in PFC^{2D}. (a) Normal component of contact force and (b) shear component of contact force.

$$\tau_f = c + \delta \tan\varphi \tag{1}$$

where τ_f is the shear strength, φ is the internal friction angle, c is the cohesion force, and δ is normal stress acting on the shear plane.

In addition to the Coulomb force, Van der Waals force, cementation force, and matrix suction, the cohesion force is also affected by the bonding force of water film. The change characteristics of cohesion force of tailing sands under the effect of water contents and DWCs are shown in Figure 8. It can be observed that in the natural water content, the cohesion force of the tailing sands is not at the maximum value. It increases first and then decreases with the increase in water content. This is consistent with the conclusions of many scholars [34–36]. The main reason for this phenomenon is that the tailing sands sample with natural water content is relatively dry, and the number of water molecules between the particles is small. The weak traction between particles does not allow the tailings particles to be firmly bonded together. With the increase in water content, the number of water molecules increases and the liquid bridge force is formed between the particles, which results in greater cohesion force. Previous studies [35] have shown that the matric suction decreases with the increase in water content. After the water content reaches 12%, the degree of cementation weakening due to the decrease of matric suction is greater than the degree of cementation strengthening due to liquid bridge force. When the water content exceeds 12%, the cohesion force of the tailing sands shows decreasing trends.

Under the condition of the same water content, the cohesion force of the tailing sands all decreased to varying degrees after the DWCs. The cohesion force decreased greatly after 1 cyclic drying and wetting and the decline trend of cohesion force became more and more gentle with the increasing number of DWCs. During the DWCs, the internal pore structure of the tailing sands became loose and the thickness of the bond water film decreased, which resulted in a decrease in cohesion force. After multiple DWCs, the internal structure and the thickness of the bond water film tend to be stable, which resulted in the cohesion force changing slowly with the increasing number of DWCs.

It can be observed from Figure 9 that the internal friction angle of the tailing sands increases first and then decreases with the increasing water content. It has a maximum value at the optimum water content (16%). Before the water content reaches 16%, the friction strength is enhanced due to the existence of liquid bridge force, which increases the traction between the particles. When the water content increases to a certain level, the water film becomes thicker and weakens the contact between the particles of the tailing sands. The lubricating effect of water on the surface of the particles makes the connection between the particles easy to break, leading to a reduction in the friction strength between the particles. The internal friction angle gradually decreases with the increasing number of DWCs. It is attributed to the change in the pore structure of the tailing sands samples after cyclic drying and wetting. The DWCs make the distance between particles larger, which leads to a decrease in friction strength. Moreover, the water inside the sample is always changing, and the water as a lubricant also has an impact on the mutual friction between the particles.

4. Numerical Analysis and Discussion of PFC

In the PFC theory, soil or rock materials are simulated as a collection of round or spherical particles that have normal and tangential stiffness. Each particle is in contact with its neighbors through a bond. There are 2 different types of contact models in PFC, namely the contact bond model and the parallel bond model [37–39]. In the contact bond model, the contact between particles can be imagined as a pair of springs with normal and tangential stiffness, which can transmit elastic interaction force at the contact point, but cannot resist the rotation and tension of the particles. In the parallel bond model, the contact between particles can be imagined as a group of springs evenly distributed on a rectangular cross-section, which is centered at the contact point on the contact surface. It can not only transmit the

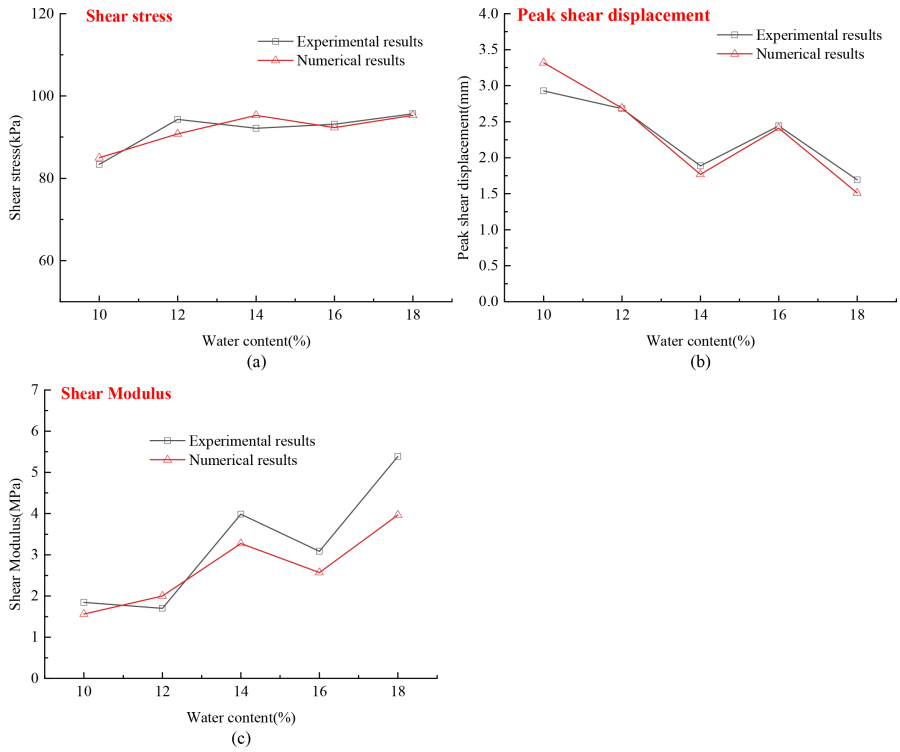

Figure 11: Comparison of experimental and numerical results of macroscopic mechanical parameters of tailing sands samples without experiencing drying and wetting cycle. (a) Shear strength; (b) peak shear displacement; and (c) shear modulus.

Table 3: Mesoscopic parameters of the numerical model.

	Values									
	Samples without experiencing DWC					Samples experiencing 5 times DWC				
Mesoscopic parameters	10%	12%	14%	16%	18%	10%	12%	14%	16%	18%
Minimum radius, R_{min}/mm	0.3									
Maximum radius, R_{max}/mm	0.45									
Density of particle, ρ/kg·m^{-3}	2000									
Effective modulus of the particle, E_c/MPa	3.5	4.5	7.8	5.8	8.8	3.5	4.8	5.05	4.76	8.8
Normal to shear stiffness ratio of particle, k_n/k_s	1.5									
Effective modulus of the parallel bond, E_c'/MPa	3.5	4.5	7.8	5.8	8.8	3.5	4.8	5.05	4.76	8.8
Normal to shear stiffness ratio of parallel bond, (k_n/k_s)'	1.5									
Cohesion of parallel bond, Pb_coh/10^5 Pa	1	1.1	1.03	1.02	1.2	0.77	0.77	0.80	0.98	1.2
Tensile strength parallel bond, Pb_ten/10^5 Pa	2	2.2	2.06	2.04	2.4	1.54	1.54	1.60	1.96	2.4

elastic interaction force between particles but also resist moment caused by rotation. In the contact bond model, the bond is broken and the contact stiffness remains valid as long as the particles remain in contact. However, in the parallel bond model, the bond broken will lead to a decrease in stiffness. The parallel bond model can better reflect the properties of soil or rock materials in reality. Therefore, the PB model was applied in our study. Figure 10 shows the constitutive behavior of the parallel bond model in PFC^{2D}.

4.1. The Particle and Model Size. The particle radius of the tailing sands is concentrated in the range of 0.125–0.15 mm, and the particle size is relatively fine. The size of the direct shear sample is Φ61.8 × 20 mm. In the process of establishing the PFC model, the using of real particle size and gradation will lead to a large number of particles, which requires high computer configuration. To facilitate modeling and improve calculation efficiency, the particle radius in the model only needs to satisfy the macroscopic mechanical properties. Many scholars have studied the influence of size effect on numerical simulation. Liu and Chen [40] found that when the ratio of the model size (L) to the average particle radius (R) is greater than 30, the size effect has the least influence on the shear

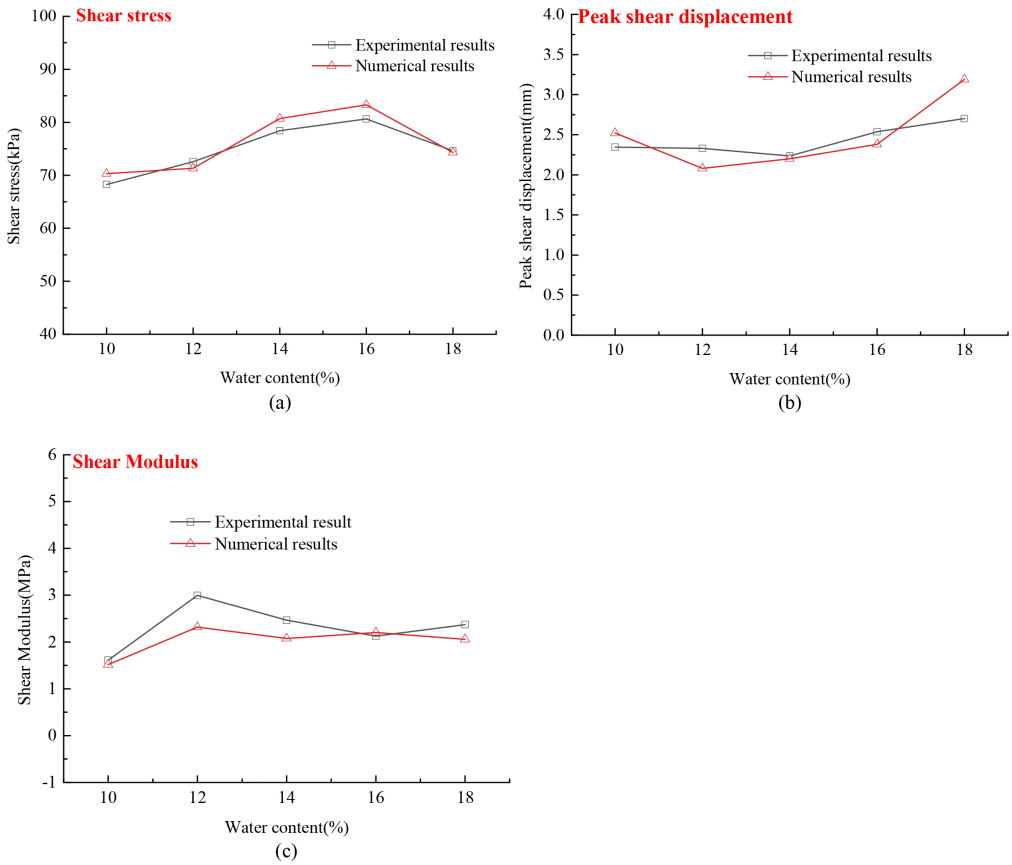

FIGURE 12: Comparison of experimental and numerical results of macroscopic mechanical parameters of tailing sands samples experiencing 5 times drying and wetting cycles. (a) Shear strength; (b) peak shear displacement; and (c) shear modulus.

strength. At the same time, the experiment data shows that the porosity of the prepared tailing sands sample is 0.336, which can be directly substituted into the calculation when using PFC^{3D} for simulation. But, for two-dimensional (2D) model, the data obtained in the laboratory should be converted. According to the conclusion of Zhou et al. [41], the transformation of three-dimensional (3D) to 2D equations is obtained as follows:

$$n_{2d} = 0.42 \times n^2 + 0.25 \times n \quad (2)$$

where n_{2d} is the porosity for 2D model and n is the porosity measured in laboratory.

Based on the above conclusions, the size of the 2D model is $\Phi 61.8 \times 20$ mm and the porosity is 0.131.

4.2. Calibrating the Mesoscopic Parameters of the Model. The particle flow simulation requires mesoscopic physical and mechanical parameters of the model. Since the transformation relationship between the mesoscopic parameters and the macroscopic parameters is very complicated, it is difficult to obtain these mesoscopic parameters from laboratory experiments. Whether the developed numerical model matches the test result depends on how the model mesoscopic parameters are calibrated. At present, the most commonly used method for calibrating mesoscopic parameters is the "trial and error method". A large number of numerical simulations with conditions similar to the indoor test were carried out before formal numerical simulation. When the data obtained from the simulation is close to the laboratory test data, it is considered that the mechanical properties of the sample obtained from the numerical model are similar to that obtained from the laboratory test. By repeatedly changing the mesoscopic parameters and verifying the corresponding macroscopic data, the mesoscopic parameters are finally obtained as shown in Table 3. The comparison results of the shear mechanical parameters obtained by the numerical simulation test and the laboratory test are shown in Figures 11 and 12. It can be seen that the shear parameters obtained by the numerical simulation method are similar to the experimental results. The particle flow numerical model can well reflect the mesoscopic mechanical behavior of tailing sands.

4.3. Force Chain Analysis. The mechanical behavior of tailing sands is mainly determined by the contact force between particles. Tailing sands are composed of thousands of particles, and the links between the particles form a complex force chain network with strength. Under the action of external force, the contact force between particles is transmitted along the force chain network. The different shapes, uneven sizes, and random distribution of tailing sands particles result in varying magnitudes of the

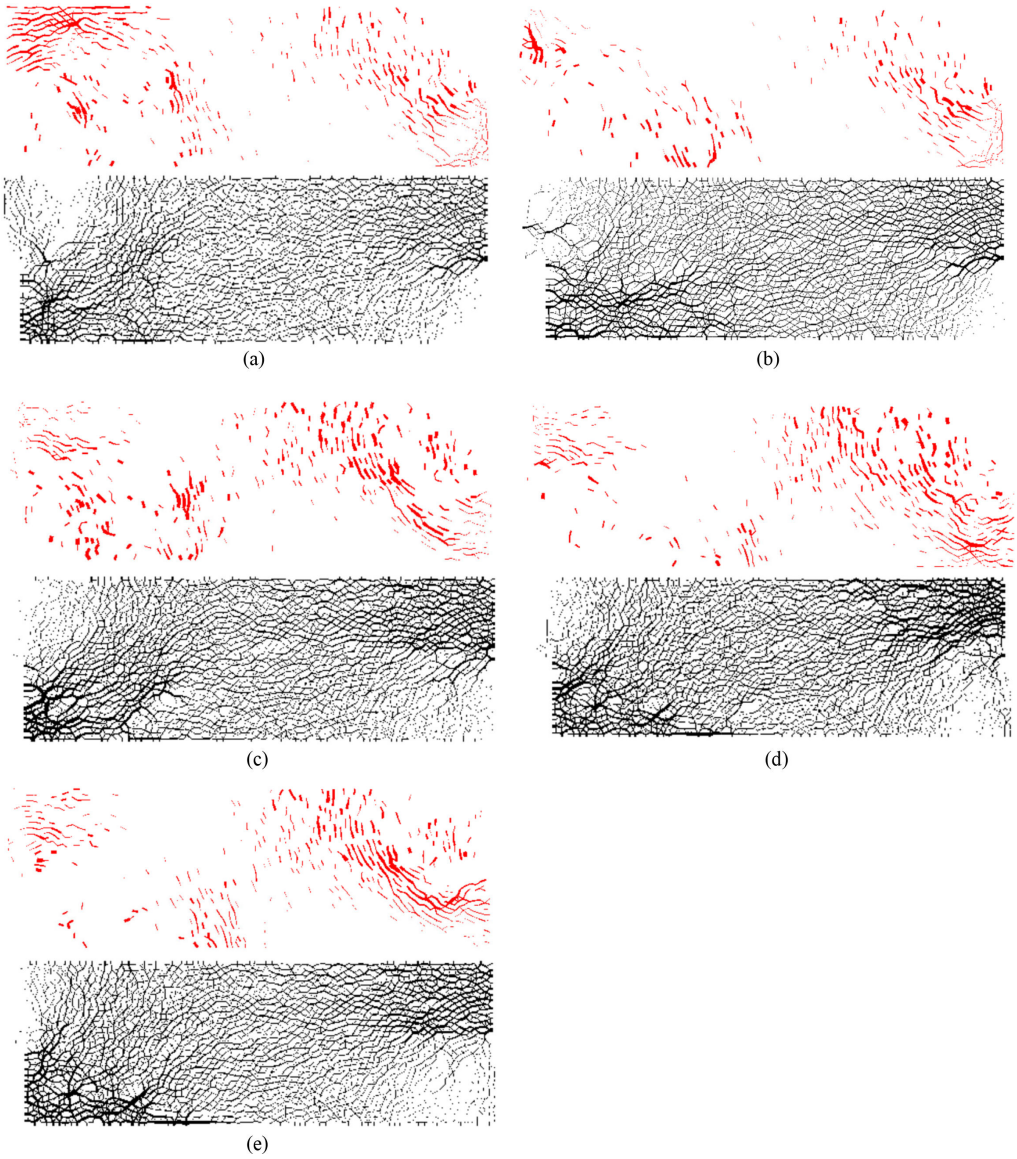

Figure 13: Distribution of force chains (tailing sands samples experiencing 0 drying and wetting cycle). (a) 10% water content; (b) 12% water content; (c) 14% water content; (d) 16% water content; and (e) 18% water content.

transmitted contact force. The formed force chain structure is staggered and scattered through the tailing sands particles. It is constantly changing under the action of external force, thus affecting the macroscopic mechanical behavior of tailing sands. With a vertical load of 100 kPa, the contact force chain network in peak shear stress state (the red is the chain under tension and the black is the chain under compression) of tailing sands samples that have experienced 0 and 5 times DWCs are shown in Figures 13 and 14.

At the beginning of shear, a velocity to the right is provided to the lower part of the direct shear box. The force chain changes from the lower left part of the shear box, and the contact force becomes larger. During the shearing process, the force chain slowly extends from the lower left corner to the upper right corner. At the peak shear stress, the force chain at the shear band is thicker and the contact force is larger. Comparing the force chain of the samples before and after the DWC, it can be seen that under the effect of DWCs, the force chain at the shear band presents an obvious tree-root distribution. The change in force chain during the shearing process can be defined as the 4 stages of occurrence, development, failure, and residual (the force chain of the samples subjected to 0 and 5 times DWCs with a water content of 18% are shown in Figure 15).

(a) At the stage of occurrence (OA section), the force chain is evenly distributed inside the sample in the shape of a fishnet, with no obvious direction. (b) The sample is subjected to continuous shear force, and the force chain enters the development stage (AB) stage from the occurrence stage (OA stage), in which the force chain presents a certain direction. It begins to show the characteristics of tree root distribution. (c) At the peak shear stress condition, it enters the failure stage (BC section). At this stage, the

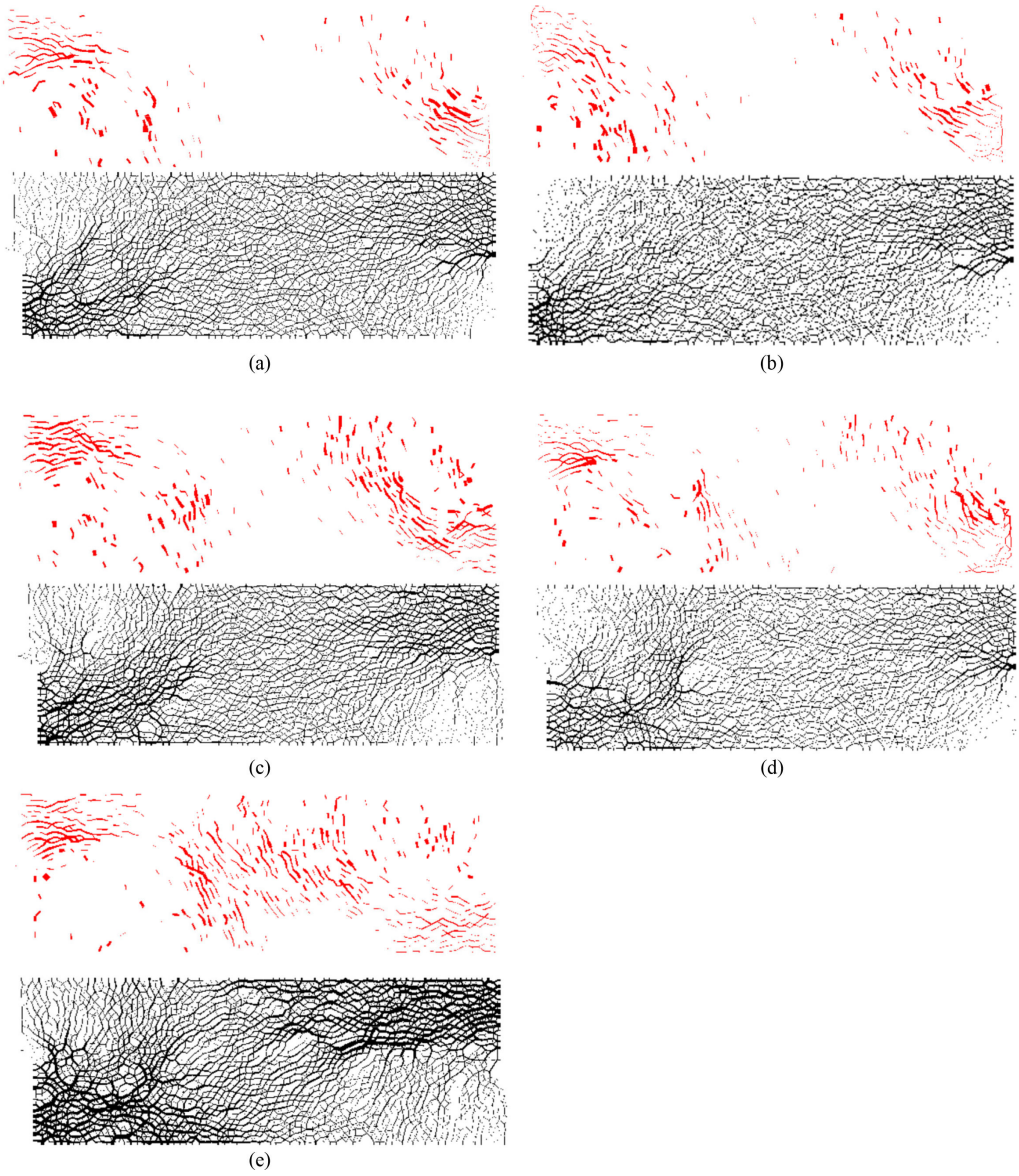

Figure 14: Distribution of force chains (tailing sands samples experiencing 5 drying and wetting cycles). (a) 10% water content; (b) 12% water content; (c) 14% water content; (d) 16% water content; and (e) 18% water content.

force chain shows obvious thickness characteristics at the crack area. At the edge of the crack area, the force chain is thicker. Due to the destruction of the bond between particles in the crack area, the force chain in this gradually becomes thinner, and the number gradually decreases. (d) At the residual stage (CD segment), due to the reduced bonding between particles in the fracture zone, the force chain is refined and the number is reduced, resulting in an obviously thicker force chain network at the boundary of the fracture zone. Especially in the failure and residual stages, the force chains near the cracks of the samples subjected to DWCs show significant differences. The force chain number and thickness of the samples subjected to the DWCs are larger than those without DWCs. In the sample, particles in a region with dense force chains bear and transmit the largest force, resulting in the formation of damage in this area.

4.4. Mesoscopic Crack Evolution Characteristics. When local stresses (i.e., moments of tension, shear, or particle rotation) applied within the sample are greater than the strength of the bonds between the particles, these bonds break and form a fracture surface. During the loading process, the relationship between the loading time step and the number of cracks inside the tailing sands sample is shown in Figure 16.

During the shearing process, the crack evolution can be divided into 3 stages, first is the stage of no cracks, the second is the stage of slow crack development, and the third is the stage of rapid crack development. In the first stage of crack development, there was no bond breakdown inside the tailing sands sample, and therefore no cracks were generated. Cracks continued to generate within the second stage, but the number of cracks was very small. In

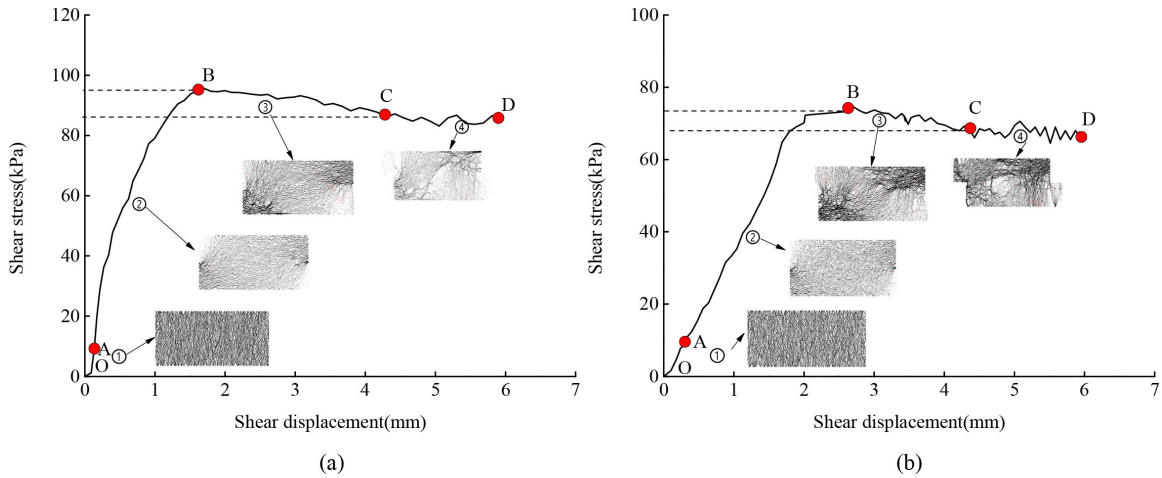

Figure 15: The phase change of the force chain. (a) Tailing sands sample experiencing 0 drying and wetting cycle and (b) tailing sands sample experiencing 5 times drying and wetting cycles.

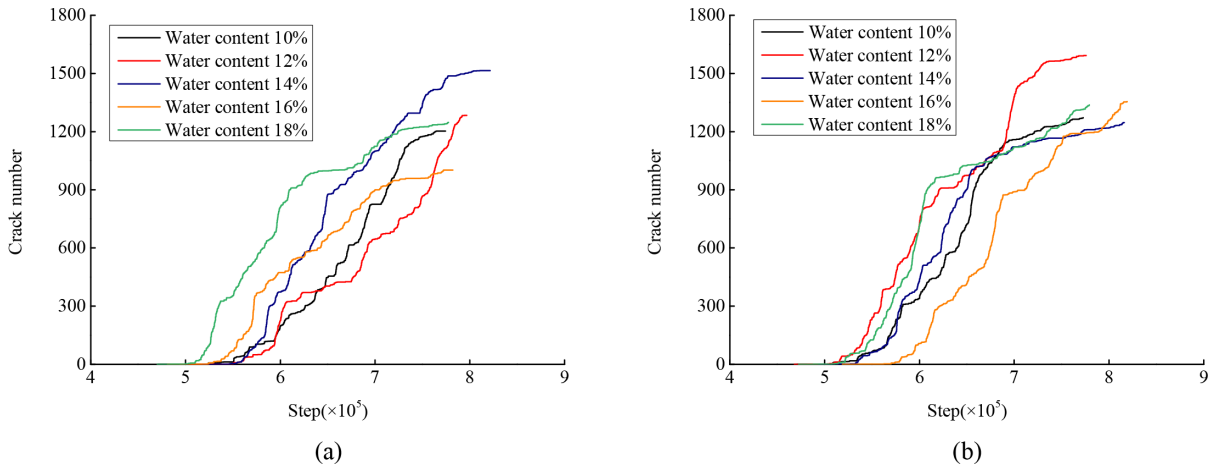

Figure 16: Relation curves between the numerical step and the crack number of tailing sands with different water content. (a) Tailing sands sample experiencing 0 drying and wetting cycle and (b) tailing sands sample experiencing 5 times drying and wetting cycles.

the third stage, the crack continued to develop, and the speed of crack propagation increased rapidly.

Under the action of DWCs, the cracks of tailing sands samples with different water content showed different evolution characteristics during the shear process (as shown in Figure 17). With the same water content, the number of cracks inside the tailing sands samples under the action of DWCs is larger than that without the DWC. In the shearing process, there are shear cracks caused by friction slip or rotation, and tension cracks caused by tension or compression. It can be seen from Figure 17 that the cyclic drying and wetting makes the samples more susceptible to shear cracking and tensile cracking during the shearing process. Except for the 14% water content condition, the number of shear and tension cracks was greater than that of the samples without experiencing wetting and drying cycles. The number of cracks in samples with different water content is different, and the influence of water content on crack evolution does not show a uniform law. Under the condition of shear failure, the number of cracks in tailing sands samples without cyclic drying and wetting are 1203 (10% water content), 1284 (12% water content), 1515 (14% water content), 1002 (16% water content), 1247 (18% water content), and the number of cracks is the largest when the water content is 14%. The number of cracks in the tailing sands samples after 5 DWCs are 1271 (10% water content), 1593 (12% water content), 1246 (14% water content), 1355 (16% water content), 1338 (18% water content), and the number of cracks is the largest when the water content is 12%

4.5. Failure Mode. After reaching the peak shear stress, the distribution of internal cracks (among which green is shear cracks caused by compression, blue is the shear cracks caused by tensile, and red is tension cracks) of tailing sands samples with different water contents under the action of cyclic drying and wetting is shown in Figures 18 and 19 .

At the beginning of the shearing process, a few cracks first formed on the central plane along the shearing direction. With the continuous application of shear stress, the sample without experiencing DWCs was subjected to greater stress in the area of the coarse force chain. The bond

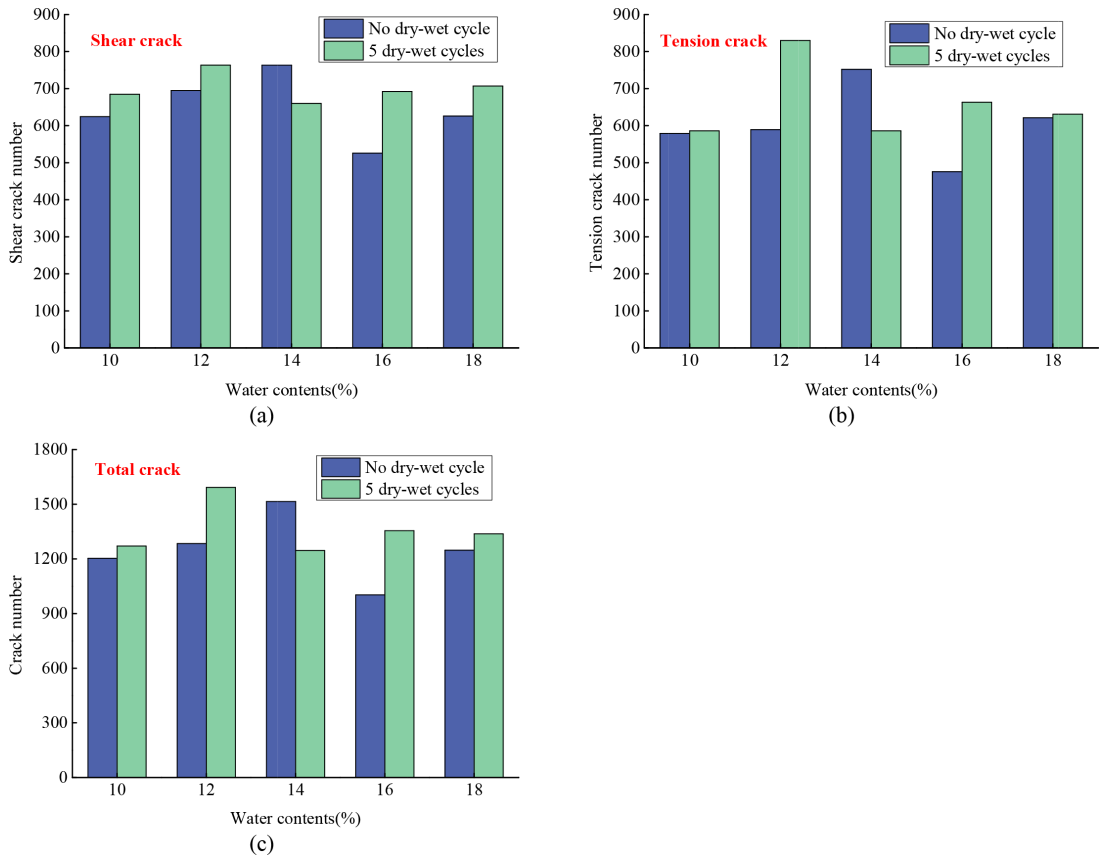

FIGURE 17: Characteristics of crack evolution of tailing sands under the effect of dry and wet cycling and water content. (a) Shear crack, (b) Tension crack, and (c) Total crack.

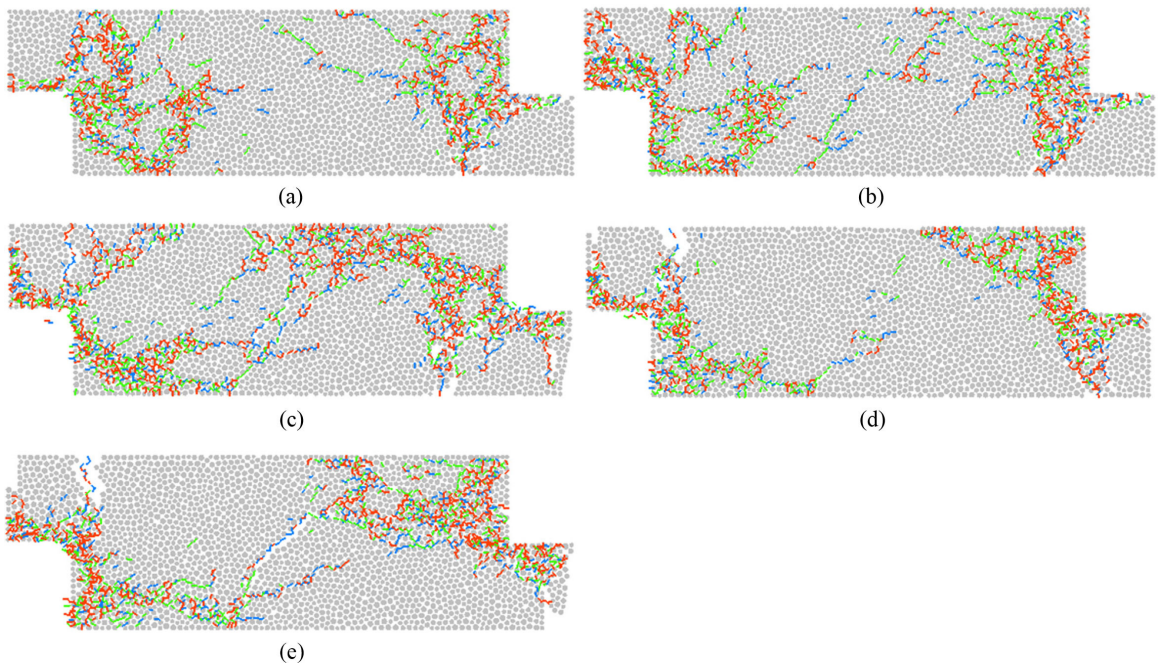

FIGURE 18: Cracks distribution of tailing sands experiencing 0 drying and wetting cycle. (a) 10% water content; (b) 12% water content; (c) 14% water content; (d) 16% water content; and (e) 18% water content.

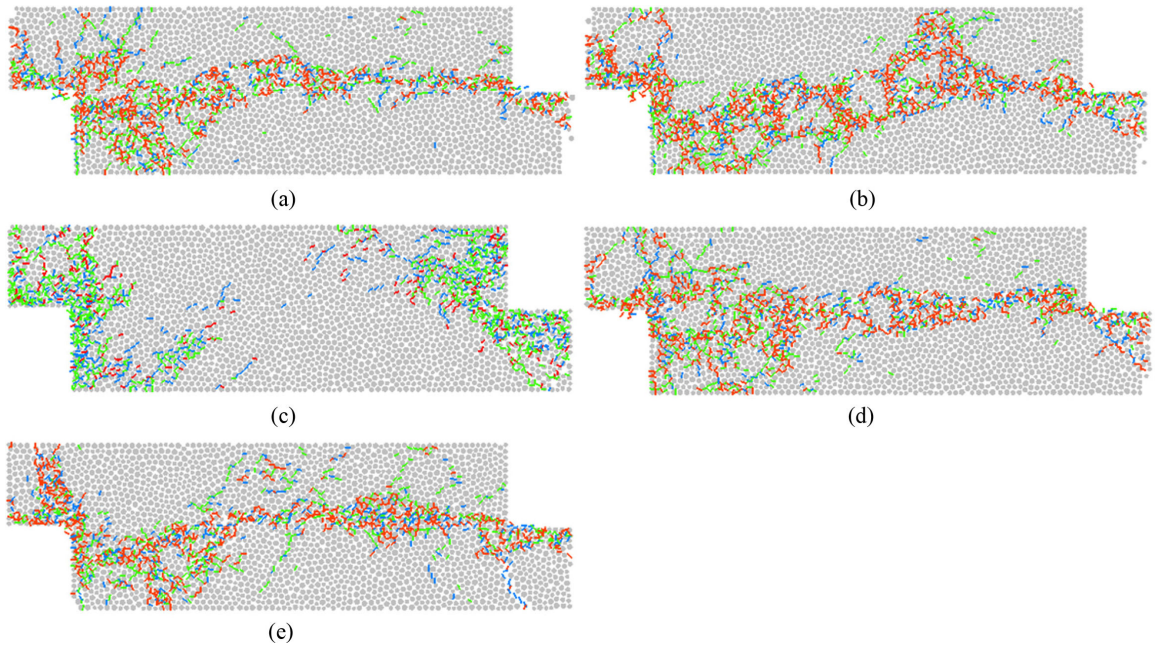

Figure 19: Cracks distribution of tailing sands experiencing 5 drying and wetting cycles. (a) 10% water content; (b) 12% water content; (c) 14% water content; (d) 16% water content; and (e) 18% water content.

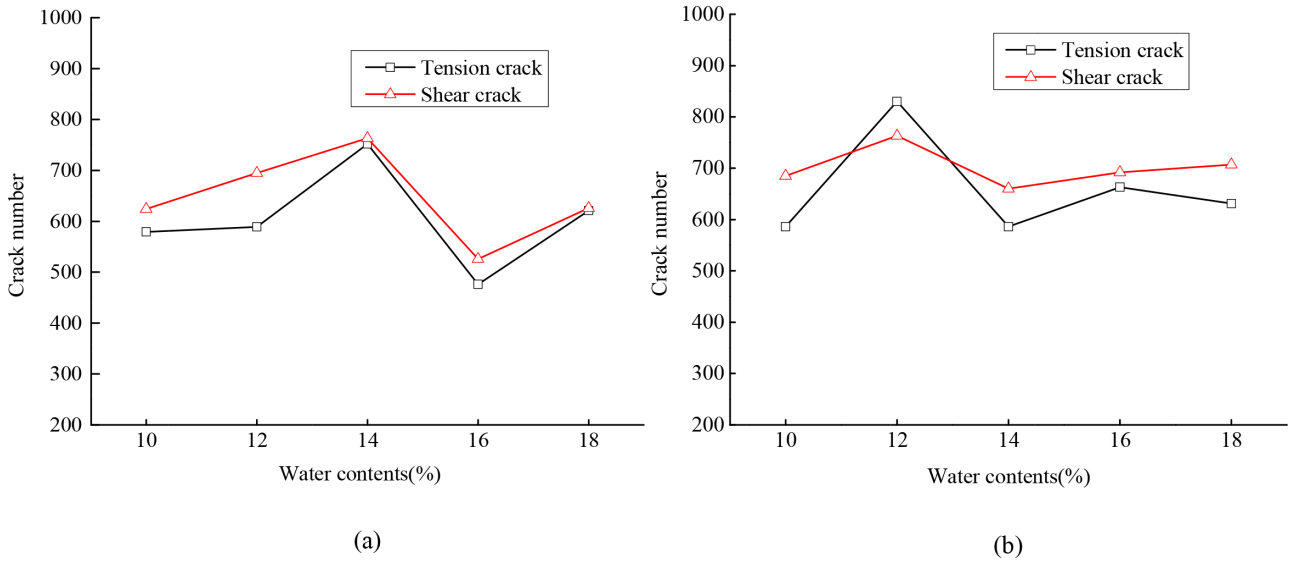

Figure 20: Comparison of the number of shear cracks and the number of tensile cracks. (a) Tailing sands sample experiencing 0 drying and wetting cycle and (b) tailing sands sample experiencing 5 times drying and wetting cycles.

between particles was destroyed and the number of cracks continuously increased, resulting in the development and penetration of cracks and eventually formed a large fracture surface. Under the action of cyclic drying and wetting, the bond force between particles weakened, and more cracks were formed at the failure surface (this is also confirmed in Section 4.4). The development of cracks led to the formation of perforated crack surfaces on the central plane of the sample. The comparison of the shear cracks and tensile cracks number in the tailing sands samples when shear failure occurs is shown in Figure 20. It can be found that the samples that have not experienced DWCs and those that have experienced 5 DWCs show the same characteristics that the number of shear cracks is greater than that of tensile cracks. The tailing sands samples exhibited a shear failure mode.

5. Conclusions

To explore the effects of water content and DWCs on the shear mechanical properties of tailing sands, direct shear tests were carried out. The changing characteristics of shear mechanical parameters under different water content and number of DWCs were analyzed. Further analysis of

the mesoscopic mechanical behavior of tailing sands was carried out by using a discrete particle flow model. Based on the above study, the following conclusions can be drawn.

(1) With the increasing number of DWCs, the shear strength decreases, and the shear displacement corresponding to the shear strength becomes smaller. At 16% water content, the shear strength is higher than other water content conditions.

(2) The cohesive force increases first and then decreases with the increase in water content. With the increasing number of DWCs, the cohesive force decreased to varying degrees. As the number of DWCs increases, the decline trend of cohesion force becomes more and more gentle.

(3) The internal friction angle increases first and then decreases with the increase in water content, and has a maximum value at optimum water content of 16%. As the number of DWCs increased, the internal friction angle gradually decreased, and the reduction rate became larger and larger.

(4) With the effect of DWCs, the force chain of the sample gradually thickens and shows obvious tree-root shape and directional characteristics. In the shearing process, the force chain of the tailing sands sample is characterized by 4 stages: occurrence, development, failure, and residual.

(5) The number of internal cracks of tailing sands samples that subjected to cyclic drying and wetting is larger than that without cyclic drying and wetting. The DWCs break the bond between the particles, making it more susceptible to internal cracking. The number of cracks in tailing sands samples with different water contents is different, but the effect on the number of cracks does not show a certain regularity.

Data Availability

The datasets generated and/or analyzed during the current study are available from the corresponding author upon reasonable request.

Conflicts of Interest

The authors declare no conflicts of interest.

Authors' Contributions

Conceptualization, Y.T. and M.W.; methodology, M.W, Z.Z, L.W, L.H, and R.G.; software, Y.T. and M.W.; validation, Y.T. and L.W.; writing—original draft preparation, Y.T. and M.W.; writing—review and editing, Y.T., M.W., Z.Z., L.W., L.H. and R.G. All authors have read and agreed to the published version of the manuscript.

Acknowledgments

This experimental work was financially supported by the National Natural Science Foundation of China(Grant No. 52274167), the Research Foundation of Education Bureau of Hunan Province (Grant No. 22B0410, 22C0221, 23A0329), the Natural Science Foundation of Hunan Province(Grant No. 2021JJ30571, 2022JJ40374, 2023JJ40549), the Hunan Province's technology research project "Revealing the List and Taking Command" (Grant No. 2021SK1050), the Science and Technology Innovation Program of Hunan Province, China (Grant No. 2023RC3171), and the Hengyang City Science and Technology Program Project Funding (Grant No. 202150063769).

References

[1] A. Özbek, "Investigation of the effects of wetting-drying and freezing-thawing cycles on some physical and mechanical properties of selected Ignimbrites," *Bulletin of Engineering Geology and the Environment*, vol. 73, no. 2, pp. 595–609, 2014.

[2] Z. H. Zhang, Q. H. Jiang, C. B. Zhou, and X. T. Liu, "Strength and failure characteristics of Jurassic Red-bed sandstone under cyclic wetting-drying conditions," *Geophysical Journal International*, vol. 198, no. 2, pp. 1034–1044, 2014.

[3] B. Y. Zhang, J. H. Zhang, and G. L. Sun, "Deformation and shear strength of rockfill materials composed of soft siltstones subjected to stress, cyclical drying/wetting and temperature variations," *Engineering Geology*, vol. 190, pp. 87–97, 2015.

[4] X. R. Liu, Z. J. Wang, Y. Fu, W. Yuan, and L. L. Miao, "Macro/micro testing and damage and degradation of sandstones under dry-wet cycles," *Advances in Materials Science and Engineering*, vol. 2016, pp. 1–16, 2016.

[5] Z. H. Zhao, J. Yang, D. F. Zhang, and H. Peng, "Effects of wetting and cyclic wetting–drying on tensile strength of sandstone with a low clay mineral content," *Rock Mechanics and Rock Engineering*, vol. 50, no. 2, pp. 485–491, 2017.

[6] Z. L. Zhou, X. Cai, L. Chen, W. Z. Cao, Y. Zhao, and C. Xiong, "Influence of cyclic wetting and drying on physical and dynamic compressive properties of sandstone," *Engineering Geology*, vol. 220, pp. 1–12, 2017.

[7] Z. L. Zhou, X. Cai, D. Ma, L. Chen, S. F. Wang, and L. H. Tan, "Dynamic tensile properties of sandstone subjected to wetting and drying cycles," *Construction and Building Materials*, vol. 182, pp. 215–232, 2018.

[8] Y. F. Zhao, S. Ren, D. Y. Jiang, R. Liu, J. X. Wu, and X. Jiang, "Influence of wetting-drying cycles on the pore structure and mechanical properties of mudstone from Simian mountain," *Construction and Building Materials*, vol. 191, pp. 923–931, 2018.

[9] S. Y. Huang, J. J. Wang, Z. F. Qiu, and K. Kang, "Effects of cyclic wetting-drying conditions on elastic modulus and compressive strength of sandstone and mudstone," *Processes*, vol. 6, no. 12, p. 234, 2018.

[10] W. M. Yao, C. D. Li, H. B. Zhan, et al., "Multiscale study of physical and mechanical properties of sandstone in three Gorges reservoir region subjected to cyclic wetting-drying of

Yangtze river water," *Rock Mechanics and Rock Engineering*, vol. 53, no. 5, pp. 2215–2231, 2020.

[11] D. M. Gu, H. L. Liu, X. C. Gao, D. Huang, and W. G. Zhang, "Influence of cyclic wetting-drying on the shear strength of limestone with a soft interlayer," *Rock Mechanics and Rock Engineering*, vol. 54, no. 8, pp. 4369–4378, 2021.

[12] P. Y. Guo, J. Gu, Y. Su, J. Wang, and Z. W. Ding, "Effect of cyclic wetting-drying on tensile mechanical behavior and microstructure of clay-bearing sandstone," *International Journal of Coal Science & Technology*, vol. 8, no. 5, pp. 956–968, 2021.

[13] X. S. Li, K. Peng, J. Peng, and D. Hou, "Experimental investigation of cyclic wetting-drying effect on mechanical behavior of a medium-grained sandstone," *Engineering Geology*, vol. 293, p. 106335, 2021.

[14] X. S. Li, K. Peng, J. Peng, and H. H. Xu, "Effect of cyclic wetting-drying treatment on strength and failure behavior of two quartz-rich sandstones under direct shear," *Rock Mechanics and Rock Engineering*, vol. 54, pp. 5953–5960, 2021.

[15] Q. R. Ke, C. D. Li, W. M. Yao, et al., "Comparative characterization of sandstone microstructure affected by cyclic wetting-drying process," *Int J Rock Mech Min*, vol. 170, p. 105486, 2023.

[16] Q. Wu, Y. X. Liu, H. M. Tang, et al., "Experimental study of the influence of wetting and drying cycles on the strength of intact rock samples from a red stratum in the three gorges reservoir area," *Engineering Geology*, vol. 314, p. 107013, 2023.

[17] W. M. Yao, C. D. Li, Q. R. Ke, et al., "Multi-scale deterioration of physical and mechanical properties of Argillaceous siltstone under cyclic wetting-drying of Yangtze river water," *Engineering Geology*, vol. 312, p. 106925, 2023.

[18] H. R. Li, Y. F. Qiao, M. C. He, et al., "Effect of water saturation on dynamic behavior of sandstone after wetting-drying cycles," *Engineering Geology*, vol. 319, p. 107105, 2023.

[19] W. Hua, S. M. Dong, Y. F. Li, J. G. Xu, and Q. Y. Wang, "The influence of cyclic wetting and drying on the fracture toughness of sandstone," *International Journal of Rock Mechanics and Mining Sciences*, vol. 78, pp. 331–335, 2015.

[20] P. Ying, Z. M. Zhu, L. Ren, et al., "Deterioration of dynamic fracture characteristics, tensile strength and elastic modulus of tight sandstone under dry-wet cycles," *Theoretical and Applied Fracture Mechanics*, vol. 109, p. 102698, 2020.

[21] X. Cai, Z. L. Zhou, L. H. Tan, H. Z. Zang, and Z. Y. Song, "Fracture behavior and damage mechanisms of sandstone subjected to wetting-drying cycles," *Engineering Fracture Mechanics*, vol. 234, 2020.

[22] S. M. Rao and K. Revanasiddappa, "Influence of cyclic wetting drying on collapse behaviour of compacted residual soil," *Geotechnical and Geological Engineering*, vol. 24, no. 3, pp. 725–734, 2006.

[23] S. G. Goh, H. Rahardjo, and E. C. Leong, "Shear strength of unsaturated soils under multiple drying-wetting cycles," *Journal of Geotechnical and Geoenvironmental Engineering*, vol. 140, no. 2, p. 06013001, 2014.

[24] I. Hafhouf, O. Bahloul, and K. Abbeche, "Effects of drying-wetting cycles on the salinity and the mechanical behavior of Sebkha soils: a case study from ain M'Lila, Algeria," *Catena*, vol. 212, p. 106099, 2022.

[25] C. S. Tang, D. Y. Wang, B. Shi, and J. Li, "Effect of wetting-drying cycles on profile mechanical behavior of soils with different initial conditions," *Catena*, vol. 139, pp. 105–116, 2016.

[26] H. D. Li, C. S. Tang, Q. Cheng, S. J. Li, X. P. Gong, and B. Shi, "Tensile strength of clayey soil and the strain analysis based on image processing techniques," *Engineering Geology*, vol. 253, pp. 137–148, 2019.

[27] C. S. Tang, Q. Cheng, T. Leng, B. Shi, H. Zeng, and H. I. Inyang, "Effects of wetting-drying cycles and desiccation cracks on mechanical behavior of an unsaturated soil," *Catena*, vol. 194, p. 104721, 2020.

[28] C. S. Tang, Q. Cheng, X. P. Gong, B. Shi, and H. I. Inyang, "Investigation on microstructure evolution of clayey soils: a review focusing on wetting/drying process," *Journal of Rock Mechanics and Geotechnical Engineering*, vol. 15, no. 1, pp. 269–284, 2023.

[29] K. Gu, C. S. Tang, B. Shi, J. J. Hong, and F. Jin, "A study of the effect of temperature on the structural strength of a clayey soil using a micro-penetrometer," *Bulletin of Engineering Geology and the Environment*, vol. 73, no. 3, pp. 747–758, 2014.

[30] N. An, C. S. Tang, Q. Cheng, D. Y. Wang, and B. Shi, "Application of electrical resistivity method in the characterization of 2D desiccation cracking process of clayey soil," *Engineering Geology*, vol. 265, p. 105416, 2020.

[31] Q. Cheng, C. S. Tang, H. Zeng, C. Zhu, N. An, and B. Shi, "Effects of microstructure on desiccation cracking of a compacted soil," *Engineering Geology*, vol. 265, p. 105418, 2020.

[32] X. G. Wang, H. B. Zhan, J. D. Wang, and P. Li, "On the mechanical damage to tailings sands subjected to dry-wet cycles," *Bulletin of Engineering Geology and the Environment*, vol. 78, no. 6, pp. 4647–4657, 2019.

[33] Z. Zhang, Y. Guo, Y. Tian, et al., "Macroscopic and mesoscopic mechanical properties of mine tailings with different dry densities under different confining pressures," *Geofluids*, vol. 2020, pp. 1–12, 2020.

[34] B. Zhang, Q. G. Zhao, R. Horn, and T. Baumgartl, "Shear strength of surface soil as affected by soil bulk density and soil water content," *Soil and Tillage Research*, vol. 59, nos. 3–4, pp. 97–106, 2001.

[35] E. Cokca, O. Erol, and F. Armangil, "Effects of compaction moisture content on the shear strength of an unsaturated clay," *Geotechnical and Geological Engineering*, vol. 22, no. 2, pp. 285–297, 2004.

[36] H.-B. Ly and B. T. Pham, "Prediction of shear strength of soil using direct shear test and support vector machine model," *The Open Construction and Building Technology Journal*, vol. 14, no. 1, pp. 41–50, 2020.

[37] D O Potyondy and P. A. Cundall, "A bonded-particle model for rock," *International Journal of Rock Mechanics and Mining Sciences*, vol. 41, no. 8, pp. 1329–1364, 2004.

[38] N. A. Cho, C. D. Martin, and D. C. Sego, "A clumped particle model for rock," *International Journal of Rock Mechanics and Mining Sciences*, vol. 44, no. 7, pp. 997–1010, 2007.

[39] P. T. Wang, F. H. Ren, and M. F. Cai, "Influence of joint geometry and roughness on the multiscale shear behaviour of fractured rock mass using particle flow code," *Arabian Journal of Geosciences*, vol. 13, no. 4, pp. 1–14, 2020.

[40] H. T. Liu and X. H. Chen, "Discrete element analysis for size effects of coarse-grained soils," *Rock and Soil Mechanics*, vol. 30, no. S1, pp. 287–292, 2009.

[41] Y. Zhou, S. C. Wu, J. J. Jiao, and X. P. Zhang, "Research on meso-mechanical parameters of rock and soil mass based on BP neural network," *Rock and Soil Mechanics*, vol. 32, no. 12, pp. 3821–3826, 2011.